

Characterization of P-static for Antenna and Receiver Design Standards

Robert Lilley, Aviation Management Associates Inc.
Robert Erikson, US Federal Aviation Administration

RIN Nav-08; ILA-37; October 28, 2008

Robert Lilley (Robert.Lilley@avmgt.com)

Dr. Lilley works with Aviation Management Associates in Washington, D.C., supporting the FAA as a consultant. He was Chief Engineer for Northrop Grumman Simulation Technologies and previously Vice President of Illgen Simulation Technologies, with responsibilities for navigation-related activities in Santa Barbara, CA, and Illgen's Washington, DC staff. Dr. Lilley is Director Emeritus of the Avionics Engineering Center, Ohio University, earned his Ph.D. at Ohio University and is an instrument-rated commercial pilot.

Robert Erikson (Robert.Erikson@faa.gov)

Robert Erikson was graduated from Drexel University with a BS in Electrical Engineering in 1973. Since graduation he has worked for the Federal Aviation Administration at the William J Hughes Technical Center in Atlantic City, NJ. Currently he is the Test Director for Loran Systems and Transponder Landing System projects at the Technical Center.

ABSTRACT

P-static is the term used to describe electrical noise which can be generated by the transport of electrical charge from the airframe to the surrounding atmosphere. Flight in clouds, precipitation or dust can result in an electrically charged airframe, and discharges from trailing edges, antenna tips and other devices.

Since the February, 2008 announcement that the U.S. will continue Loran services and deploy *eLoran*, emphasis has increased on development of standards for *eLoran* antennas and receivers for aviation. Recent high-voltage measurements conducted at the U.S. FAA Technical Center reveal detail about the discharge mechanisms, and point the way to affordable standard test configurations for proponent antennas.

KEYWORDS

Precipitation static, p-static, corona, airframe dischargers, e-field and h-field antennas, Loran, *eLoran*.

INTRODUCTION

Throughout the U.S. Federal Aviation Administration's (FAA) Loran-C and more recent *eLoran* programs, concern has been voiced over *precipitation static* or *p-static* noise effects on system availability and navigational accuracy. P-static is the term used to describe electrical noise

which can be generated by the transport of electrical charge from the airframe to the surrounding atmosphere. Flight in clouds, precipitation or dust can result in an electrically charged airframe, with subsequent ion-avalanche (corona) discharges from trailing edges, antenna tips and other devices.

The most recent FAA guidance on p-static effects is Advisory Circular (AC) 20-121A [1], released in 1988 and still in effect. E-field "whip" antennas were standard practice then, and the agency included installation and maintenance advice to minimize navigational outages due to precipitation static. This was not entirely successful, and although Loran-C retains instrument-flight approval in en-route and terminal-area airspace, non-precision approach use was only briefly available at specially-equipped destinations. The advent of Required Navigation Performance (RNP) placed tighter accuracy, availability, integrity and continuity requirements on systems proposed for use in the National Airspace System. Enhanced Loran (*eLoran*) was born of these necessities.

Since the February, 2008 announcement [2] that the U.S. Department of Homeland Security will continue Loran services and deploy *eLoran*, development of standards for *eLoran* antennas and receivers for aviation has received increased interest and emphasis. Recent ground and flight measurements conducted at the W. J. Hughes FAA Technical Center (FAATC) for the FAA Loran

Program, apply directly to the development, test and approval of *eLoran* user equipment. This work is designed to reveal detail about p-static discharge mechanisms, offer suggestions for minimization of p-static noise at the antenna, describe the residual noise voltage which may appear at the receiver terminals, and point the way to affordable standard signals and acceptance tests for proponent antennas.

P-static (corona) discharges are not “just more noise.” The results to date confirm the *pulsed* nature of corona discharge and the “tunable” pulse repetition rate. While the repetition frequencies have been observed over a range of frequencies, the narrow pulse geometry produces broad spectral content, some of which enters the receiver bandpass during each corona pulse occurrence. This paper offers a status report and description of work in progress at the FAATC, where a flight test program and a high-voltage laboratory are characterizing the p-static phenomenon in preparation for U.S. RTCA guidance and approval documents for *eLoran* avionics.

A description of *eLoran* and its differences from Loran-C can be found in the International Loran Association’s “Enhanced Loran (*eLoran*) Definition Document.” [3] The description includes the statement “Most *eLoran* aviation receivers employ so-called *H-field* (or, magnetic loop) antennas. Extensive tests have shown that these antennas are almost immune to the effects of the Precipitation Static (p-static) experienced during flight in rain and snow, which has been a problem for users of traditional Loran-C airborne receivers.” This paper outlines work in progress to characterize and accommodate p-static.

AIRFRAME-GENERATED ELECTRICAL NOISE

The airframe is an isolated conductor on which stored charge increases with time as charged particles are encountered, when “triboelectric” charging occurs upon impact with rain/snow/dust particles, or when friction between air and engine parts causes charge separation. Faster, larger aircraft naturally encounter more particles, resulting in higher charging rates. Observed aircraft charging rates approach 400 μA for light general-aviation aircraft, up to 750 μA for cabin-class twins, and as high as 1.5 mA for airliners. Currents of 5 mA have been recorded in extreme cases. [4] Three mechanisms account for unequal potential among airframe components and between the airframe and its surroundings:

Arcs: Arcs can occur when airframe components become charged to different potentials across non-conductive gaps, which can occur due to corrosion or loose components. Arcs cause broadband noise and are relatively energetic.

Streamers: Streamers are low-current arcs which travel across dielectric surfaces --windscreens, radomes and composite components. Special conductive treatments on these surfaces can reduce streamer noise and lightning effects. The effects of streamers are similar to arcs.

Corona: Although not uniquely energetic among the noise sources, corona can be uniquely troublesome due to its pulsed, periodic nature, which results in interference which can be “tuned” over a wide range of frequencies. [5]

Loran receivers can be affected by all three types of interference. We emphasize corona discharge in current work, to prompt discussion of its unique frequency-selective effects which may require specific receiver and antenna considerations.

Corona Discharge

When the airframe is charged, the equalization of this charge occurs at the trailing edges (and antenna tips and other convenient spots), as ions of opposite polarity are attracted to the points on the aircraft with small radii of curvature (the points where maximum electric field intensity exists for a given airframe potential). When a conducting element reaches the electric-field corona threshold, atmospheric breakdown (ion avalanche) occurs as free atmospheric ions are accelerated to the point where they in turn ionize neutral air atoms. A chain reaction results, causing the air to change almost instantly from an insulator into a conductor, and “breakdown” occurs. The slipstream removes ion products and replenishes the corona-point region for the next avalanche event. The resulting current pulse (Figure 1) is very short, producing significant spectral content reaching from the repetition frequency to well above VHF.

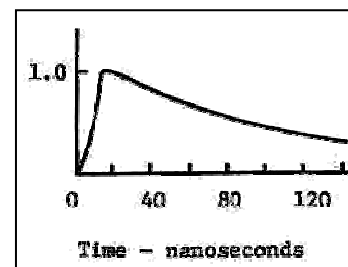


Figure 1: Corona pulse [4]

Once initiated, the discharge is quenched by the momentary increase of the effective radius of the discharge point by the ion charge cloud produced by the avalanche. The discharge also removes stored charge from the airframe, reducing momentarily its electric field. The pulse-to-pulse electrical *amplitude* of these corona discharge events is nearly constant, determined by the characteristics of the surrounding air temperature, pressure (altitude), humidity, and the aircraft's velocity, all of which affect the air ionization process. When airframe charge and the resulting electric field increase, the *repetition rate* of the corona discharges, not their amplitude, increases.

EARLIER WORK

The FAA Technical Center ground electrostatic survey and flight measurements [6] and laboratory tests to date confirm similar work at Ohio, 1982; [7,8] Illgen in 1999; [9] and Ohio in 2004. [10, 11] The survey data also agree broadly with uncontrolled or anecdotal observations of p-static interference reported by pilots, e.g. Edwards [12] and others. The three different instrumented aircraft (DC-3, PA-32 Saratoga and Aero Commander) tested in the FAA programs since 1982 exhibit some consistency [13] in the quantity of p-static noise generated by a given flow of discharger current, in both ground and flight measurements. This noise consistency over dissimilar airframes encourages development of a general standard, rather than installation-specific approvals for avionics including *eLoran* functions.

E-field Comparisons Among Aircraft

For all three aircraft tested, "quieting" the airframe by greater than 20 dB using purpose-built trailing-edge static dischargers was demonstrated (See Table 1).

Noise @ 100 μ A	DC-3	Saratoga	Aero Cmdr
Bare aircraft	33.9 dB	28.1 dB	24.0 dB
With dischargers	4.5 dB	2.6 dB	1.0 dB
Difference	29.4dB	25.5 dB	23.0 dB

Table 1: Ground test p-static noise at Loran frequency: - 100 μ A current, e-field antennas.

Well-designed e-field antennas may be successful in these quieted circumstances, *provided* airframe and discharger maintenance programs are followed, avoiding corrosion, discharger burnout, or degradation over time.

The similarities in Table 1 are striking when one considers the different airframe size, shape, and different percentage of aluminum and non-conductive skin and structure among the aircraft tested over the years. It appears that the total discharge current may be a better predictor for p-static noise effects than is the aircraft type.

We are encouraged to recommend the installation of discharger devices designed to quiet the airframe at low frequencies. These provide large benefits even *before* we consider using h-field "loop" antennas to optimize *eLoran* performance.

H-Field Antenna Benefits

The modern receiver using an h-field "loop" antenna shows greater than 20 dB (some measurements indicate up to 50 dB [10]) more "protection" from p-static noise than does the same receiver using an e-field antenna. Even at levels of charge/discharge considered "severe" in aviation experience, there was little or no p-static reduction of signal-to-noise ratio (SNR) using receivers with h-field antennas.

Figure 2 shows the benefit clearly, from an FAA ground test on the Aero Commander Aircraft in August, 2004 with receivers operating on a simulated West Coast Loran chain. As the airframe is charged and discharge current increases (lower right) to over 140 μ A (a moderate to high discharge level in practice), a "legacy" hard-limited receiver using an e-field antenna stops navigating almost immediately upon p-static onset (top curve, black; not calibrated). The lower curve (blue) reveals the steady reduction of SNR for a modern-design Loran receiver using an e-field antenna. Station tracking stops on the third, and then the second station in the chain (lower left and upper right chart panels).

Throughout the test, the receiver with the h-field antenna (middle curve, red) was unaffected by the increase in discharge current (and noise). The momentary change in h-field SNR somewhat above 50 μ A of discharge current is unexplained, but does not occur in other test data with the same configuration.

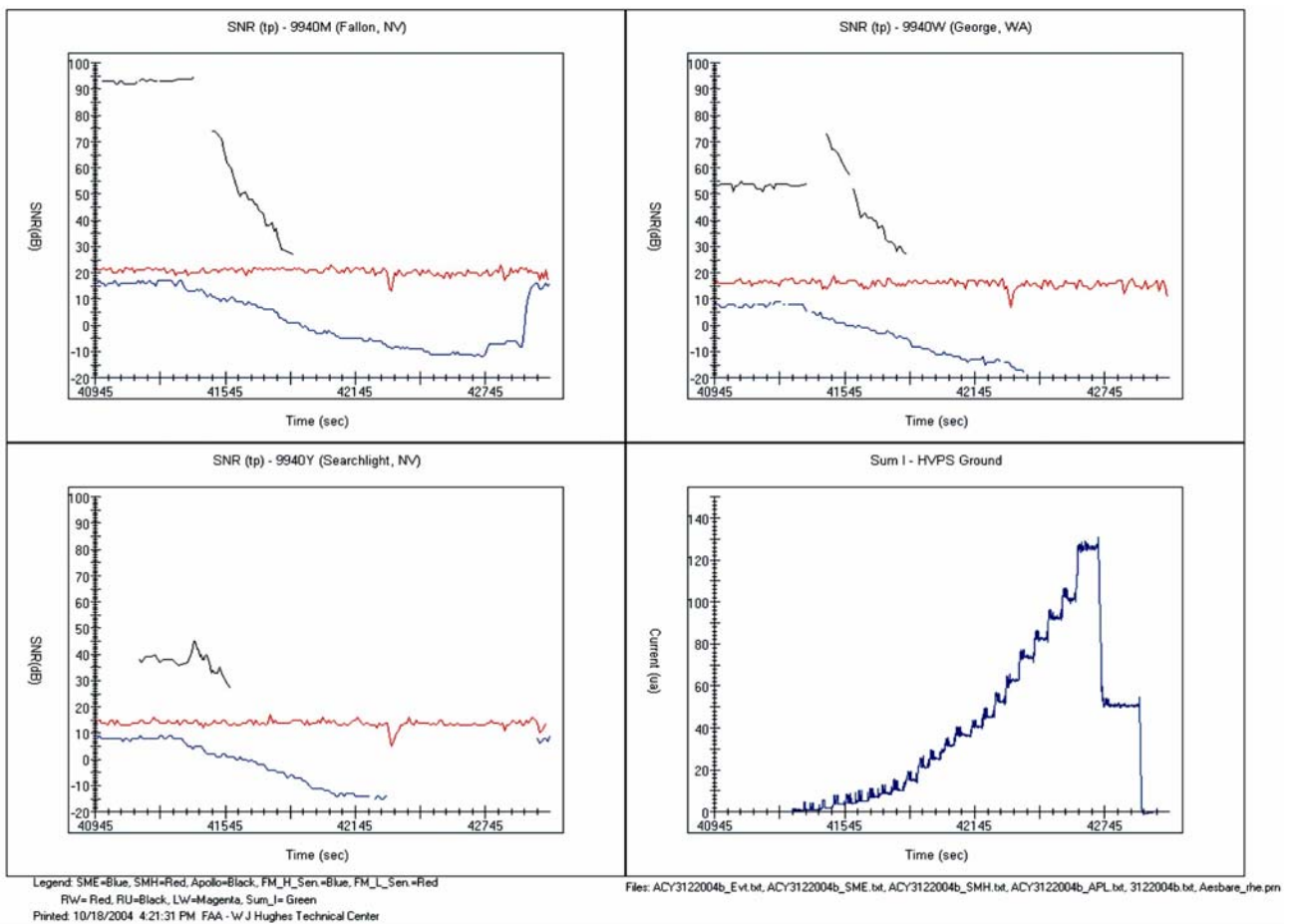


Figure 2: N50 SNR data for simulated 9940M signals vs. and discharge current; metal rod discharge points.

RECENT ACTIVITY

Flight Test Analysis

Flight measurements have continued when conditions permit. The project plan included flights with an active charging system aboard the aircraft, so that “p-static on demand” could be generated, and data could be collected in clear air. This active discharger was fabricated in earlier work, and is available at the FAATC when flights can be scheduled. Its use will improve knowledge of the charge stored on the aircraft, removing the confounding effect of charged surroundings during flight in weather.

P-static weather conditions are elusive, often occurring in weather (airframe icing, turbulence, etc.) which makes data collection difficult. To date one of the most interesting encounters is the flight

on March 25, 2004, which gave useful data for inclusion in the FAA Loran report to the U.S. Department of Transportation [11]. Figure 3 shows the encounter with airframe-charging conditions with three instrumented TCO, Inc., DD-2 dischargers installed on wing and vertical stabilizer tips. Outside conditions were favorable (i.e. mostly uncharged) for e-field measurements to determine aircraft potential. Corona onset threshold was observed to be -9,500 volts, consistent with the same discharger units in ground tests. This threshold was exceeded on two occasions, resulting in discharge current. Good agreement with ground data was observed, confirming the ground calibration methodology. Effects on e-field and h-field antennas feeding onboard Loran receivers also agreed with ground calibration measurements using the same discharger configuration, and are discussed further in [6].

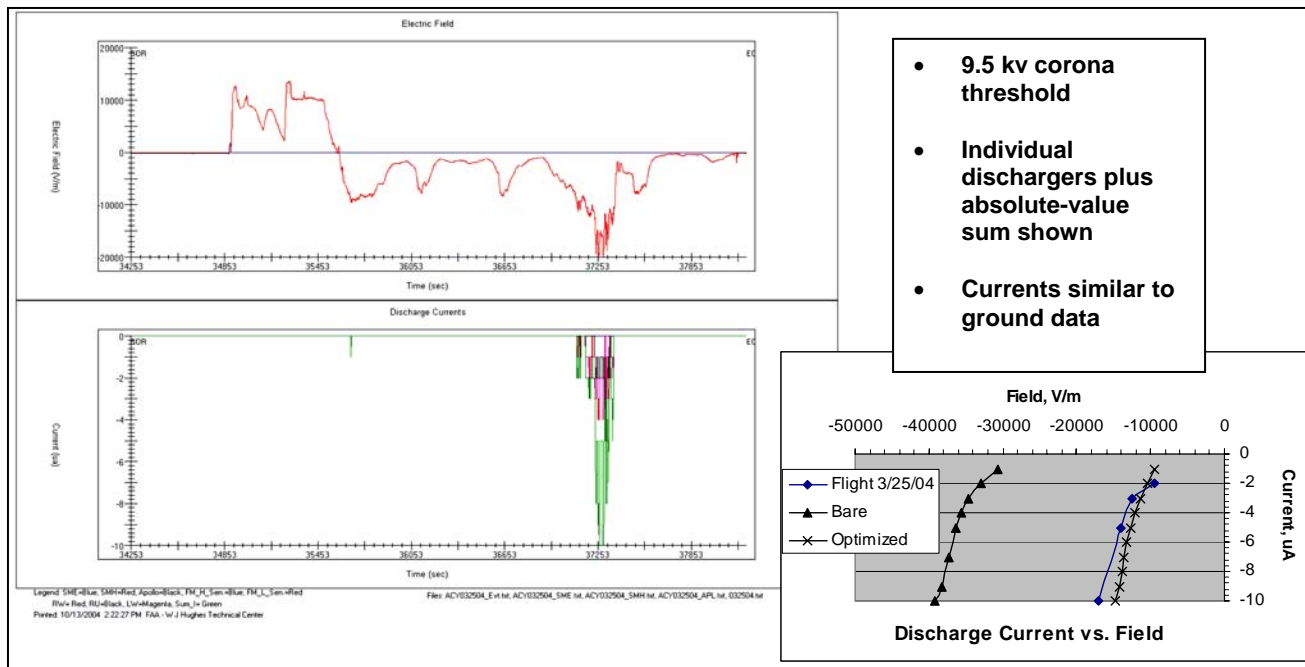


Figure 3: In-flight p-static encounter 3/25/04 with comparison to ground survey data. [13]

FAATC High-Voltage Laboratory

One of the recommendations of earlier work [14] is to “bring the measurements down to the ground,” for a more controlled test environment, better data stability and more accessibility, as elements of a MOPS acceptance-test sequence. The FAATC High Voltage Laboratory [15] meets this need, using the unique high-voltage equipment on loan from TCO, Inc. and used in earlier work. Significant knowledge was obtained on the character of p-static noise, through analysis of ground and airborne measurements and previously-collected data.

As proponent *eLoran* avionics begin to appear, it will become necessary to test receivers and antennas to develop or confirm performance. The knowledge gained during ground and flight tests of Loran-C antennas and receivers will be valuable, but eventual RTCA MOPS standard-signal and test definitions will require simpler and less expensive methods. An understanding of the details of p-static effects is necessary, to guide antenna and receiver design and acceptance testing. Ultimately, a “standard test signal” will be needed, as part of RTCA MOPS for *eLoran* avionics.

A draft laboratory test plan [16] was prepared, as a guide for tests in the FAATC anechoic chamber and the laboratory. Identification of necessary resources was begun. The laboratory equipment configuration is a subset of the full-aircraft ground electrostatic survey reported in earlier work. [6] The high-voltage equipment on loan from TCO, Inc. was configured to place a charge on an isolated wing section. TCO ion collectors at the wing’s trailing edge draw off discharge products and simulate the slipstream. As the design proceeded, Consultant Robert Truax worked with the team on a safe and effective configuration and on use of the equipment. Data recording and display methods were the same as those used in the full-aircraft ground survey. Equipment was selected from the inventory of TCO hardware on site. [17]

In addition to the TCO equipment, the test wing section and custom support stands were built. The team purchased an electric-field meter (a duplicate of the “field mill” device used to measure e-field intensity on the test aircraft), and a spectrum analyzer with computational capabilities for detailed data capture and analysis.

The wing section (Figure 4) was locally fabricated, and the FAATC anechoic chamber (Figure 5) was identified as a site for experimentation.



Figure 4: FAATC's John Tatham and Scott Shollenberger fabricate the wing section for high-voltage experimentation.



Figure 5: Anechoic chamber, FAATC hangar.

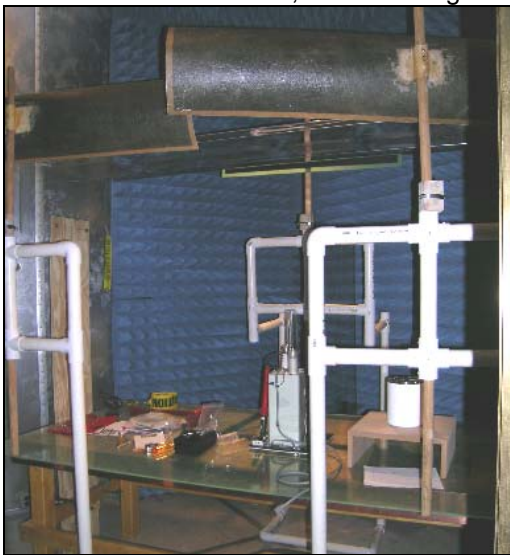


Figure 6: FAA-fabricated stands support ion flood and collector equipment surrounding the wing section in the anechoic chamber.

System components were interconnected and safety procedures established (Figure 6). Calibration of the field mill (Figure 7) and data collection system (Figure 8) were carried out at the anechoic chamber location.

Tests were carried out in the anechoic chamber from which useful data were collected, but it quickly became evident that the chamber construction was interfering with the experiments. The interior walls are covered with conductive foam "cones" which serve to absorb electromagnetic energy, resulting in the echo-free environment necessary for antenna testing. The high-voltage system charged the foam, which was mounted to the conducting walls and ceiling by non-conductive plywood. As a result, the foam retained the charge, and the resulting "room potential" interfered seriously with the accuracy of field-mill electric-field measurements.

Our work was more in need of a "screen room" to isolate us from outside signals. The anechoic chamber accomplished this, but the charged-foam problems prompted a move to another laboratory room at the FAATC hangar building (Figure 9). This location was, in fact, more electrically noisy, but early observations demonstrated that we could separate the relatively few signals from nearby radio stations from the 100 kHz signals and harmonics we were observing. Stray ions still caused charging of some objects in the room, but with installation of a peripheral ground strap, most of the "room effect" observed in the anechoic chamber was eliminated.



Figure 7: FAATC's Scott Shollenberger prepares the high voltage power supply to calibrate the field mill (right).



Figure 8: Outside the anechoic chamber, FAA Technical Monitor Robert Erikson sets up the high-voltage monitor panel, PC for data recording and the spectrum analyzer.



Figure 9: Laboratory with high-voltage equipment installed. Wing section with ion flood and collectors is visible at right, isolated by non-conducting supports. High-voltage power supply is out of sight behind the instrument cart. Note the peripheral ground wire which limits charging of room contents.

We tested the laboratory's ability to provide real-world conditions. MIL-STD-464 [18] gives an estimate of discharge currents ranging from 94 to 756 μA for the FAA's Aero Commander N50 with a frontal area of $\sim 6.3 \text{ m}^2$ used in flight tests. Our

laboratory wing is estimated at 4 ft^2 with corresponding expected charge rates from 7 to 44 μA . However, the flood circuit available in the laboratory, can exceed these rates considerably, producing real-world charge rates on demand. When we ground-tested N50, Loran receiver e-field SNR reduction with eventual loss of station track was observed with total discharger current ranging from 19 μA to 130 μA using multiple 3 mm brass rods. An N-50 flight on August 16, 2004 (Figure 10) with 3mm rod dischargers showed e-field SNR effects at as low as 5 μA , and a 20+ dB reduction with a 23 μA total current.

Consistent data from simulation and flight have demonstrated that 3mm discharge points with as little as 20 μA of discharge currents are sufficient to interfere significantly with Loran reception with an e-field antenna. The laboratory equipment will generate this and more severe charging conditions.

WORK IN PROGRESS

Earlier work emphasized ground-based emulation of flight in p-static conditions using ground tests on entire airplanes. [13] Comparing those measurements of signal-to-noise reduction in Loran receivers to in-flight data offered an opportunity to demonstrate the effects of airframe and discharger maintenance, discharger placement and other "bulk" effects of airframe-generated noise.

The return to the laboratory allows us to follow-up those earlier measurements with emphasis on quantifying the more detailed characteristics of the p-static phenomenon. Details of the summary tests reported here are preserved in the form of logs and summaries prepared by Robert Erikson and are preserved in Appendixes to the Final Report for the FAA Cooperative Agreement which supported the work. [19]

Laboratory Configuration:

Figure 11 illustrates the laboratory's arrangement, based largely on the TCO high-voltage equipment. The airframe is emulated by an isolated wing section, to the trailing edge of which various discharger elements may be attached. See Figure 9 for an overview photograph.

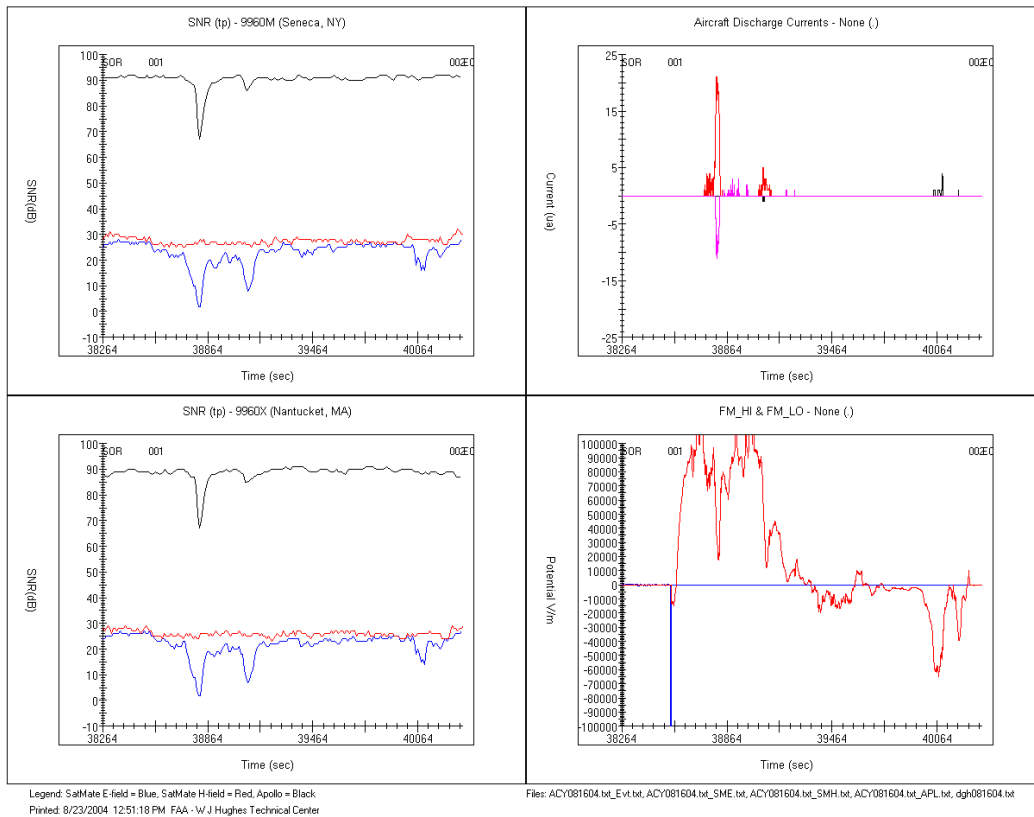


Figure 10: N50 August 16, 2004 flight showing p-static discharge current and simultaneous effects on legacy and e-field receivers. H-field receiver is unaffected.

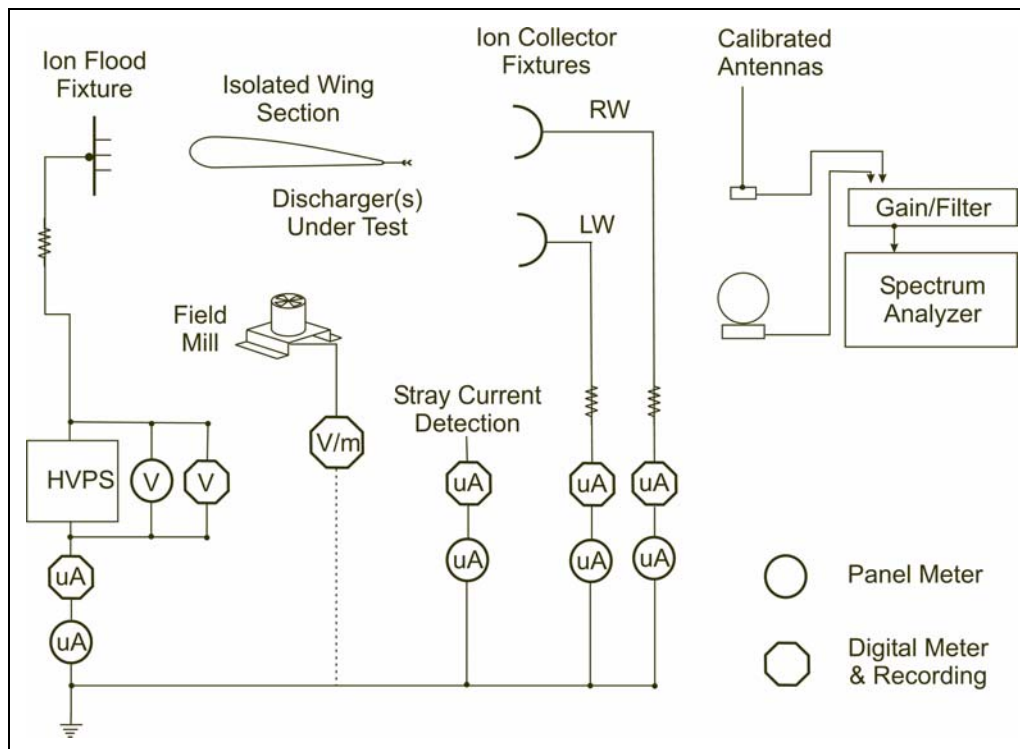


Figure 11: High-Voltage Laboratory Diagram.

Airframe charging is emulated by a high-voltage power supply which floods the leading edge of the wing section with ions released by aviation dischargers operated “in reverse.” The charge imparted to the wing raises its potential, which can reach 50 kV or higher. The wing potential is detected by the field-mill, which measures electric-field intensity in volts/meter, scaled to volts by its 1-meter separation from the wing.

One of TCO’s contributions to the art was the design of the ion collectors, placed aft of the wing and dischargers. These are resistive-coated, curved glass-fiber surfaces which serve to remove ion products from the vicinity of the discharger without distorting the electric field. They therefore emulate the in-flight slipstream. The collectors are instrumented so that current flow from individual dischargers can be measured.

Currents and voltages throughout the configuration are instrumented as shown, including metering of surfaces where stray leakage currents might occur. In our laboratory, these include the acrylic end-plates for the wing, the supports for the flood and collector units, and the peripheral ground strap which prevents incidental charging of room contents.

The measurement methods closely resemble the whole-aircraft tests performed earlier. [6] The laboratory equipment produces charge and discharge currents which are in the range already encountered in flight and in whole-aircraft ground measurements.

Test Discharger Descriptions

The corona discharge described above is the central focus of the work. On aircraft, discharger devices are used to release accumulated charge into the slipstream, reducing the potential on the airframe. It is desired that this discharge threshold potential be low enough to keep other, uncontrolled, airframe elements from going into corona. For example, an antenna in corona very likely will create unacceptable levels of interference in the associated avionics.

To produce corona at specific locations for testing, metal rod discharge points were attached to the trailing edge of the wing section. For many of the tests to date, a 3.1 mm diameter rod (Figure 12, lower) with tip rounded (Figure 13) was chosen, as this is the same device used in earlier airplane tests to emulate an airframe component (metal

edge or vent pipe, etc.) which becomes a corona point when the airframe is charged. Several smaller-diameter rods and wires (2.0mm, 1.6mm, 1mm, 0.6mm and a #30 AWG wire) were fabricated for confirmation of the decreasing corona threshold vs. radius.



Figure 12: Discharger types.

Two types of commercially-available dischargers were also included in testing, as these are popular discharger units used in the fleet. The Dayton-Granger unit (Figure 12, top) is a high-speed “orthodecoupled” discharger, with corona points placed at right angles to the trailing wing edge and with rigid construction. The discharger just below it is a TCO Inc. DD-2 discharger, often used on smaller aircraft. It has a flexible resistive body with hundreds of 4-micron wires (Figure 14) – hundreds of corona points which evidence low threshold voltage.



Figure 13: 3.1 mm rod discharger detail



Figure 14: TCO, Inc. DD-2 discharger detail

Corona Pulses: P-Static Interference

In reviewing the results of discharger tests, it must be remembered that time domain data were recorded with the spectrum analyzer set to a center frequency of 100 kHz and resolution bandwidth of 50 kHz. These values were chosen to be similar to a Loran receiver. Use of a wider resolution bandwidth would increase the fidelity of the pulse shape but would also increase the analyzer noise floor, making pulse detection more difficult.

According to Robb [5], p-static pulses have a typical rise time of 13 ns and a fall time of 179 ns. The spectrum needed to preserve such a pulse shape is very large. The actual pulse shape one observes will therefore be determined by the frequency response of the system used for measurement. Because p-static is a pulsed signal and not continuous, spectral lines will be produced as a function of pulse spacing. Using MatLab to perform fast Fourier analysis has shown that pulse repetition frequencies (PRF) as low as a few kilohertz still produces spectrum in the Loran band. As the PRF is increased, the number of spectral lines within a given band pass will

decrease. It is these spectral lines that produce a noise pulse which could affect a Loran receiver.

Measurement of PRF should not be affected by the limited bandwidth, but it was not practical to use frequency response for testing to describe the pulse shape. Measurement of amplitude and width should only be viewed in a general sense at this stage.

P-static is illustrated in the amplitude-vs.-time trace of Figure 15. This particular test was performed with a single 2mm rod discharger carrying 10 μ A of discharge current. The repetition rate seen here (roughly 10 kHz) is a product of the continuous charge rate applied to the wing section by the high-voltage power supply and the flood fixture, simulating encounters with rain, snow or dust during flight. Changing the flood current easily and continuously “tunes” the average discharge repetition rate.

The constant amplitude of the discharge pulses is evident, as is the fairly coherent interval between pulses. The pulse shape is modified from the corona pulse shown earlier due to passage through the analyzer’s passband.

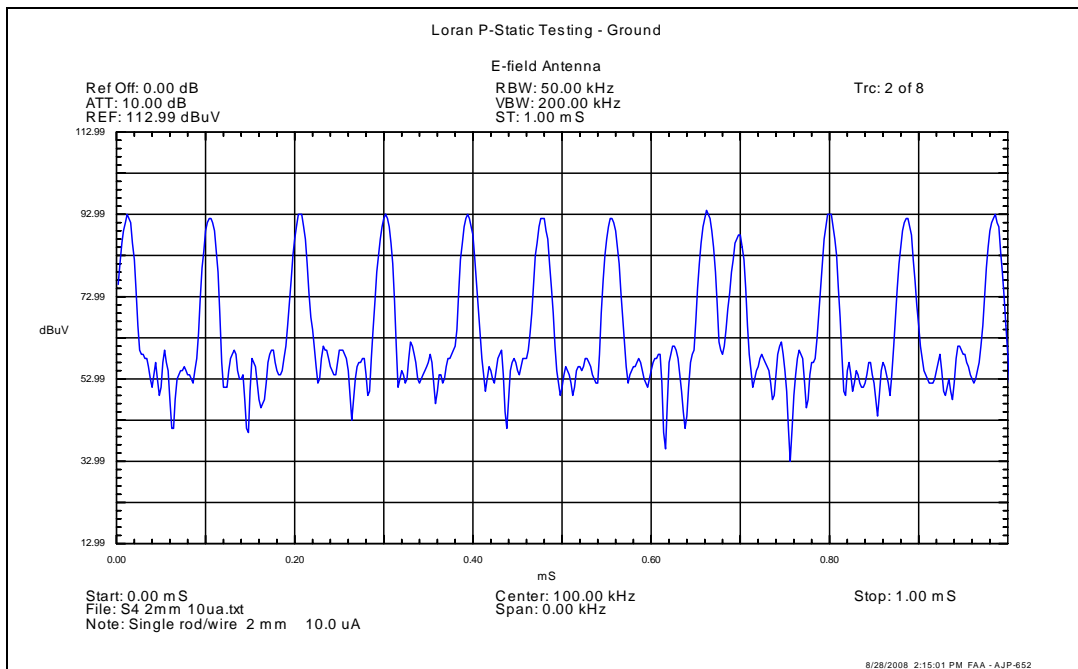


Figure 15: P-static pulses as measured with the standard, passive e-field antenna connected through the 40dB gain stage. A 2mm discharger with 10 μ A of discharge current was used for the capture. An as yet unexplained “double pulse” appears which could result from an occasional arc event somewhere in the system, or a more complicated discharger phenomenon.

Multiple Dischargers

Tests in the laboratory compared with earlier measurements during whole-aircraft calibration suggest that multiple dischargers share the task of shedding charge from the aircraft, and that the two dischargers produce independent pulse trains, resulting in the total discharge current being a predictor of total noise. Evidence comes from the laboratory test using one and two dischargers, and from the multiple-discharger configuration used to create Figure 2, which shows ~6 dB noise increase when total discharge current was doubled. Adding a second discharger in laboratory tests does affect the PRF of the first discharger; the quantitative effect is presently being characterized.

Wing potential by Discharger Type

Figure 16 shows the wing field intensity (voltage) versus discharger currents for the various discharger types tested. The metal rod with the largest radius requires higher wing potential for a given discharge current, and the commercial DD-2 unit resulted in the lowest potential for a given current -- as expected, given its very small corona-point wires. The Dayton-Granger (DG) design includes two corona points of undetermined radius, believed to be larger than the DD-2 wires.

More tests are planned on the DG discharger to confirm or modify its unexpectedly high placement in Figure 14, since the “orthodecoupled” design is specifically recommended by FAA [1], and there is at least one literature reference [20] which questions the effectiveness of the design.

For the conditions of Figure 16 to exist, the various dischargers must remove charge from the wing at different rates. Corona events occur when the breakdown field intensity of the atmosphere is reached. With a smaller discharge-point radius this threshold field intensity is reached at a lower wing voltage (at a smaller stored charge). Each corona event carries approximately the same charge transport, determined by the surrounding atmospheric conditions. Therefore, for corona current (charge transport per unit time) to increase during airframe charging, the number of corona discharge events per second must increase.

This graph shows the basic benefit of a discharger and hints at successful design. Dischargers with very small corona points hold the airframe at a lower voltage which discourages streamers and arcs, and also prevents corona noise from other pointy parts – such as antennas.

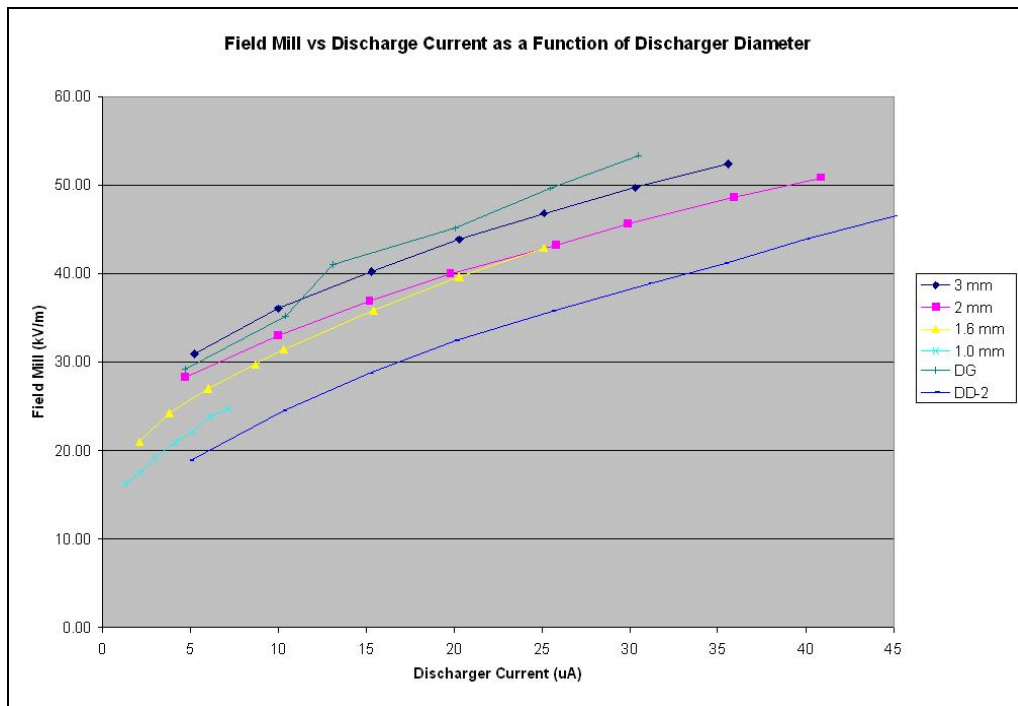


Figure 16: Wing voltage vs. discharger current as a function of discharger diameter.

Corona Event Repetition Rate

Using e-field measurements, corona pulses were observed over a range of currents for the various dischargers. As expected, PRF rises as current increases, since the current we measure is really the charge transported per unit time by corona events. Figure 17 shows PRF vs. current for the various diameter dischargers. The figure shows that as the diameter of the discharger is decreased, the amount of discharge current needed to create a given PRF is also decreased. Once the PRF exceeds ~60 kHz, time-domain identification of the pulses were quite difficult with present test implementation. Partly for this reason, the 0.6 mm and 30 AWG diameter dischargers were not tested.

Note that PRF for the 3mm rod rises nearly linearly with current, and that the increase is consistent with the whole-airplane test shown in Figure 2, showing ~6dB drop in SNR for current (and PRF) doubling.

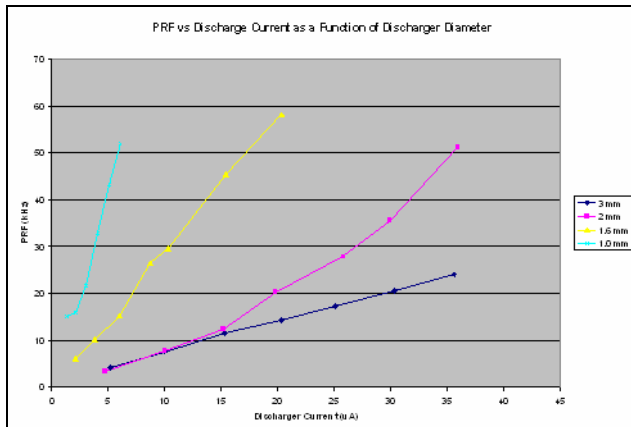


Figure 17: Corona repetition rate vs. discharge current as a function of tip radius

Corona Current Pulse Amplitude

We tested pulse amplitude as a function of discharge current for each discharger diameter. The amplitude of each individual pulse shows no significant trend as current (repetition rate) increases for a given tip radius (See Figure 18). The amplitude of the pulses remained fairly constant for a given diameter discharger but decreased with smaller discharger diameter.

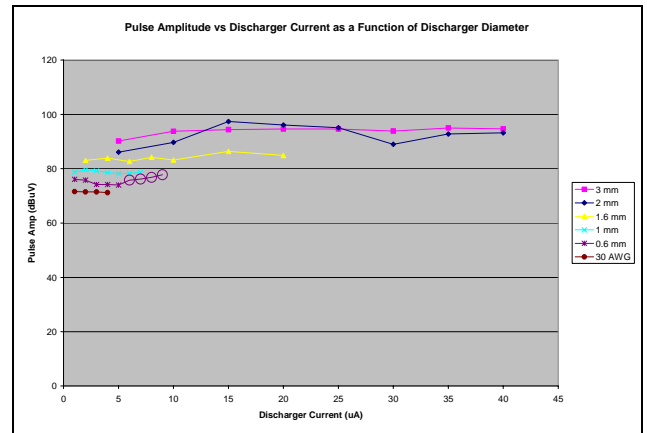


Figure 18: Pulse amplitude vs. discharger current as a function of diameter

Pulse width vs. PRF

Each corona discharge from a specific discharger is essentially like the others. We observed pulse width variations using the analyzer's 50 kHz bandpass filter. However, our preliminary tests indicated that the pulses are narrower for smaller discharge-point diameter. Also it tends to become even narrower as PRF increases. The change is small but similar regardless of diameter.

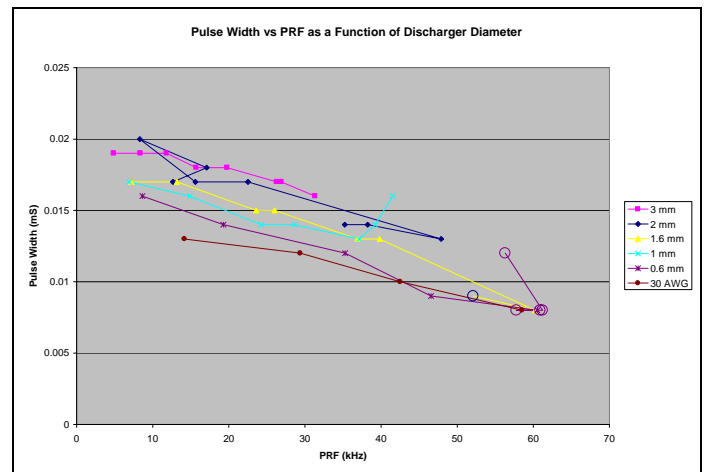
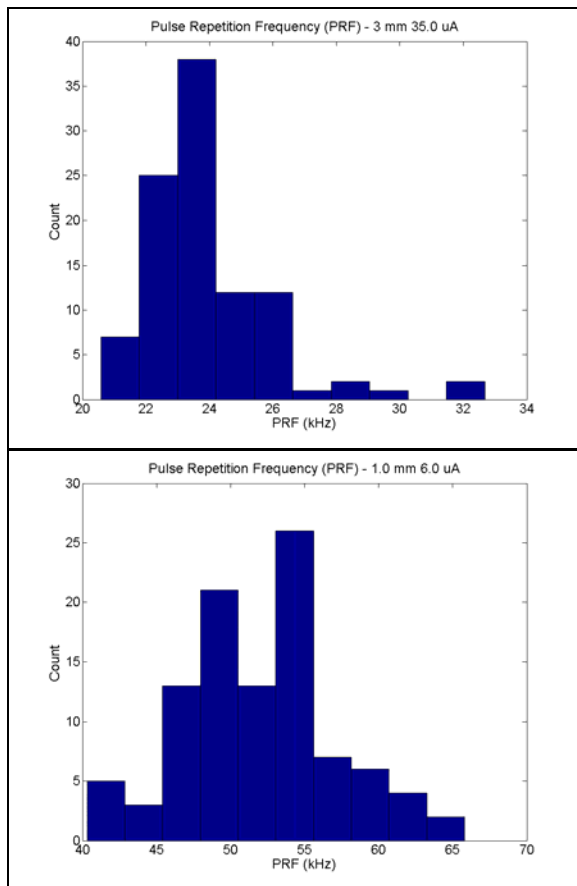


Figure 19: Pulse width vs. PRF as a function of discharger diameter

Corona PRF Coherence: Receiver Issues

Corona PRF stability may be an issue for receivers. A very stable pulse train containing 100 kHz components could either blank or confuse tracking logic. Preliminary experiments show that the standard deviation (STD) of the PRF does rise with increasing discharge current. Histograms in Figures 20 and 21 show the distribution of pulse interval length for two discharger diameters and two currents. These distributions are still under investigation, for several reasons. Observations of STD variation with diameter are suspect; the STD may not be the best descriptor if the distributions are far from Gaussian. The distributions may be influenced by small irregularities in the tip geometry, especially for the smaller-diameter dischargers. Finally, future work is expected to show the extent, large or small, to which the receiver needs to accommodate some portion of the p-static energy, and the accurate description of p-static PRF coherence is an important element of that determination.



Figures 20 and 21: Sample histograms for dischargers with different diameter and current flow.

P-Static Intensity vs. Distance

The e-field portion of this test was performed using the standard whip antenna (Figure 22). The 3 mm diameter brass rod was used as the discharger. The discharge current was set to 25 μ A, an operating point which previously demonstrated a consistent corona pulse repetition frequency with pulses that were easily detected. The external filter with 40 dB gain and the spectrum analyzer were used to measure the field. The antenna was moved in increments away from the discharger. At each location the pulse amplitude was measured by averaging 100 pulses. Note in Figure 22 that the p-static e-field measurements neatly fit within the $1/r^2 - 1/r^3$ region, as expected for near-field conditions. In the small laboratory room, there are variations in field intensity with small antenna movements orthogonal to the measurement direction, indicating that future open-field measurements or tests in a large anechoic chamber are necessary to extend the curves.

The next phase of the intensity vs. distance characteristic is to make direct measurements of the h-field. To date, p-static pulses have not been observed using h-field or "loop" antennas. The reason has not been determined. The amplitude of p-static pulses has been measured as 30 dB stronger than the strongest Loran signals in the Atlantic City. These measurements used the same e-field antenna, gains, and bandwidths. Magnetic and electric field strengths are generally related as a function of free space impedance, assumed to be a constant. Based on this assumption, if the e-field increased by 30 dB, the h-field should also have increased. During the measurement of on-air Loran signals, the noise was observed to be 14 or 35 dB below the peak of the Loran pulse depending on the h-field antenna used. This means a magnetic field some 65 dB below the expected value should have been observable.



Figure 22: Standard h-field and e-field antennas

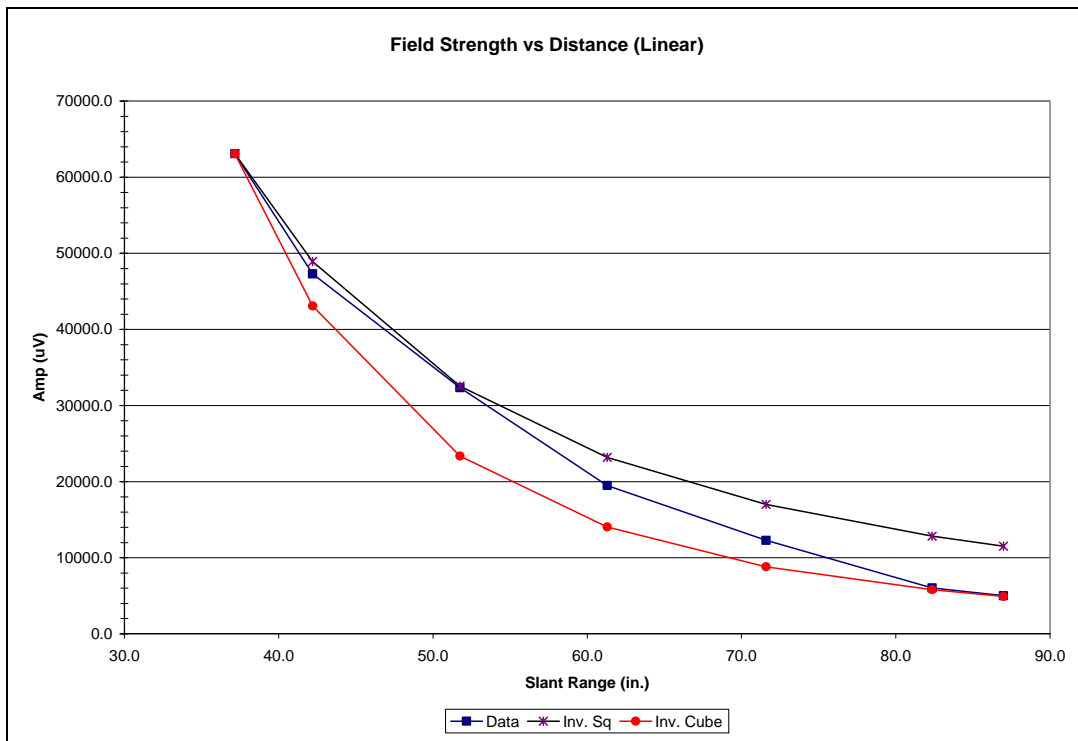


Figure 22: Corona pulse amplitude vs. distance with e-field standard antenna.

FINALLY,

As *eLoran* deployment continues, the time will come when approval standards for *eLoran* avionics (RTCA MOPS receiver and antenna documents, in the U.S.) will be needed to guide avionics approval in the NAS. Support for these documents will come from the work reported here, and from many other sources. Documents to support standards development are currently being prepared. [21]

The p-static tool-kit and knowledge base being developed at the FAA Technical Center combined with the work of the Antenna subgroup of the Loran Performance Panels [22] will be brought to the RTCA process, and to the *eLoran* community through the open literature. We now fully expect that for *eLoran*, magnetic-field antennas will be *de rigueur* to obtain necessary performance. If we understand the p-static source in both the e- and h-field domains, we can design optimal performance standards for these antennas and for any necessary receiver accommodation of residual p-static.

CONCLUSIONS

Using the FAA Technical Center laboratory, we can create realistic p-static interference conditions on demand. Using commercial-grade dischargers or simulated airframe corona-points, the corona-pulse repetition rate may easily be “tuned” by varying the charging rate.

A simulated airframe and proven methods similar to those used in past electrostatic-survey work produced example corona pulses occurring at non-random intervals, producing pulses with amplitudes that are greater than 6 dB above the field strength of the strongest Loran stations received in the Atlantic City area.

The corresponding h-field pulse amplitude has yet to be determined with a standard antenna, and the prf stability is under further study.

Pulse repetition can be increased continuously from zero to 100 kHz and much higher, even in moderate charging conditions from metal tips as large as 1-3 mm. (In fact, the rate also could be “tuned” to occur near 30, 90, 150 and 9960 Hz and beyond, all frequencies of great interest to navigation avionics designers.) Note that considerable in-band energy is available in the lower harmonics of the repetition rate, so that

interference could occur at 100 kHz with lower corona rates.

Multiple discharge points appear to share the outgoing current at repetition rates determined by their individual radii of curvature. Smaller wire points result higher repetition rates at corona onset – a phenomenon still under study. With very small discharge points, the rates can occur well above the 100 kHz band even with very low airframe charge rates, and the amplitude of the interference within the Loran band is decreased.

At completion, this work will establish e- and h-field interference levels as a function of distance from corona discharge points. Recommendations will be made for performance of antennas intended for use in instrument flight. If significant p-static interference is predicted to reach the receiver using either an e-field or h-field antenna, that interference will be described in detail, to guide signal-processing designers.

ACKNOWLEDGEMENT

Work reported here was accomplished with support from FAA Cooperative Agreements 04-G-040 and 06-G-001 with the guidance of Program Manager Mitchell Narins, FAA AJW-41. FAA Technical Center personnel Scott Shollenberger and Andre Ramjattan assisted throughout the work.

REFERENCES

[1] Federal Aviation Administration AIR-120, "Airworthiness Approval of Loran-C Systems for Use in the U.S. National Airspace System (NAS) and Alaska," Advisory Circular A/C 20-121, August 24, 1988.

[2] U.S. Department of Homeland Security, Press Office, "Statement from DHS Press Secretary Laura Keehner on the Adoption of National Backup System to GPS", Washington, D.C., February 7, 2008 document, visited October 15, 2008.

[3] "Enhanced Loran (*eLoran*) Definition Document," Version 1.0, Version Date: 16 October 2007.
<http://www.loran.org/ILAArchive/eLoran%20Definition%20Document/eLoran%20Definition%20Document-1.0.pdf> visited October 15, 2008.

[4] Truax, Robert, "Electrostatic Charging and Noise Quieting", Dayton Aircraft Products, Inc,

Lightning and Static Electricity Conference, December, 1970, Paper #700926.

[5] Robb, J. D., "ILS/VOR Navigation and Approach Errors From Precipitation Static Interference," Lightning and Static Electricity Conference, USAF Avionics Lab, Wright-Patterson AFB, Ohio, December, 1972, AFAL TR-72-325.

[6] Lilley, R., Erikson, R. "FAA tests E- and H-Field Antennas to Characterize Improved Loran-C Availability During P-Static Events," Task 1 Final Report, FAA Cooperative Agreement 04-G-040, Aviation Management Associates, Inc., Springfield, VA and W.J. Hughes FAA Technical Center Atlantic City, NJ, August 9, 2005.

[7] Nickum, J. D., "The Effects of Precipitation Static and Lightning on the Airborne Reception of Loran-C (Volume 1 - Analysis)," Ohio University, Report DOT/FAA/RD-82/45-1, 1982.

[8] Nickum, J. D., "The Effects of Precipitation Static and Lightning on the Airborne Reception of Loran-C (Volume 2 - Data)," Ohio University, Report DOT/FAA/RD-82/45-2, 1982.

[9] Lilley, Robert; Cohen, Robert; Poppe, Dorothy; "Loran-C in Support of the National Airspace System: Modeled and Experimental Results," Illgen Simulation Technologies, Inc., Report IST99-R-217, FAA contract DTFA01-97-Y-01003, Delivery Order 004, April 1999.

[10] Van Graas, F.; Diggle, D.; Cutright, C.; Lad, M.; "Loran-C P-Static," in [11].

[11] Federal Aviation Administration, "Loran's Capability to Mitigate the Impact of a GPS Outage on GPS Position, Navigation, and Time Applications," Report to the U.S. Department of Transportation, March 2004, [www Access](http://www.faa.gov), visited: October 15, 2008

[12] Edwards, Jamie S., "Results of Preliminary Flight Evaluations Comparing the Performance of h-field and e-field Loran-C Antennas in the Presence of Precipitation Static," Avionics Engineering Center, Ohio University, presented at the 29th Annual Convention, International Loran Association, Washington, DC, November 12-15, 2000.

[13] Lilley, R., Erikson R. "FAA tests E- and H-Field Antennas to Characterize Improved Loran-C Availability During P-Static Events," 33rd Annual Convention and Technical Symposium,

International Loran Association, Tokyo, Japan, October 27, 2004. Conference paper and presentation, visited October 15, 2008.

[14] Lilley, R., Erikson, R. "FAA tests E- and H-Field Antennas to Characterize Improved Loran-C Availability During P-Static Events," 2005 National Technical Meeting, Institute of Navigation, San Diego, CA USA, January 27, 2005 – Conference paper and presentation.

[15] Lilley, R., Erikson, R., "High-Voltage: P-static Test and Evaluation Facility at the FAA Technical Center," Briefing presented at ILA-35, International Loran Association, Groton, CT., October 24, 2006.

[16] Lilley, R., Draft 3: "High-Voltage Laboratory and Aircraft Test Descriptions," Aviation Management Associates, Inc., July 22, 2007

[17] Lilley, R., "Inventory of High-Voltage Equipment from TCO, Inc.," Aviation Management Associates, Inc., Effective February 24, 2006

[18] U.S. Department of Defense, "MIL-STD-464," Electromagnetic Environmental Effects: Requirements For Systems, AMSC A7252 AREA EMCS, 18 March 1997.

[19] Lilley, R., Erikson, R., "Technical Support for FAA Evaluations of Navigation Systems: Loran Augmentation of GPS in the NAS," Final Report, FAA Cooperative Agreement 04-G-040, Aviation Management Associates, Inc., Springfield, VA and W.J. Hughes FAA Technical Center, Atlantic City, NJ, September 28, 2008

[20] Newman, M., Robb, J., "Equivalent Field Method for Testing Aircraft Static Dischargers," Lightning and Transients Research Institute, Minneapolis, MN, January, 1962, NTIS Accession Number: AD0271432.

[21] (DRAFT) "Minimum Operation Performance Standards for enhanced Long Range Navigation (*eLoran*) Airborne Active Antenna Equipment," Ohio University, October 31, 2008,

[22] Bartone, C., Narins, M., Pelgrum, W., Lilley, R., Chen, L., "H-field Antenna Considerations for *eLoran* Aviation Applications," Presented at IEEE/ION Plans, Monterey, CA, May 5-8, 2008.